

URTeC: 2886597

Quantitative Interpretation Efforts in Seismic Reservoir Characterization of Utica-Point Pleasant Shale – A Case Study

Satinder Chopra*¹, Ritesh Sharma¹, Hossein Nemati¹, James Keay²

1. TGS, Calgary, 2. TGS, Houston.

Copyright 2018, Unconventional Resources Technology Conference (URTeC) DOI 10.15530/urtec-2018 2886597

This paper was prepared for presentation at the Unconventional Resources Technology Conference held in Houston, Texas, USA, 23-25 July 2018.

The URTeC Technical Program Committee accepted this presentation on the basis of information contained in an abstract submitted by the author(s). The contents of this paper have not been reviewed by URTeC and URTeC does not warrant the accuracy, reliability, or timeliness of any information herein. All information is the responsibility of, and, is subject to corrections by the author(s). Any person or entity that relies on any information obtained from this paper does so at their own risk. The information herein does not necessarily reflect any position of URTeC. Any reproduction, distribution, or storage of any part of this paper by anyone other than the author without the written consent of URTeC is prohibited.

Abstract

Utica shale is one of the major source rocks in Ohio and extends across much of eastern US. Its organic richness, high content of calcite, and development of extensive organic porosity makes it a perfect unconventional play and has gained the attention of the oil and gas industry. The primary target zone in the Utica includes Utica, Point Pleasant, and Trenton intervals. In the present study, we attempt to identify the sweet-spots within the Point-Pleasant interval using 3D seismic data, available well data, and other relevant data. This has been done by way of organic richness and brittleness estimation in the rock intervals. The organic richness is determined through TOC content which is derived by transforming the inverted density volume. The core-log petrophysical modeling provides the necessary relationship for doing so. The brittleness is first derived using rock-physics parameters such as Young's modulus and Poisson's ratio, and considering the importance of mineralogical information, we derive brittleness from this information as well. Deterministic simultaneous inversion along with a neural network approach are followed in order to compute rock-physics parameters and density using seismic data. The consistency of sweet spots identified based on the seismic data with the available production data emphasize the integration of seismic data with all other relevant data.

Introduction

The Utica shale is considered a source rock for oil and natural gas, which migrated upwards and were produced by conventional means in the overlying rock formations. According to a 2012 USGS report, the formation holds 940 million barrels of oil and approximately 38 tcf of natural gas (Kirschbaum et al., 2012), but with more drilling and production, these estimates have been revised and stand at 2 billion barrels of oil and 782 tcf of natural gas (Cocklin, 2015). The thermal maturity studies in the Utica shale have indicated a northeast to southwest trend over eastern Ohio and western Pennsylvania, with a western oil phase window, a central wet gas phase window and an eastern dry gas phase window.

We present our attempts at seismic reservoir characterization of the Utica – Point Pleasant package in eastern Ohio. Beginning with a discussion about the data that are available for the exercise, next we describe the workflow that is followed. The goal of seismic reservoir characterization is essentially the identification of sweet spots that represent the most favorable drilling areas. Such an exercise entails understanding the elastic properties of the reservoir intervals, lithology, fluid content and their areal distribution. A good starting point for doing this is to use the available well data and understand the parameters that populate the reservoir intervals at the location of the wells. The sonic, density, gamma ray, resistivity, porosity well log curves are sought for the available wells over the 3D seismic volume. Core analysis results, geochemical as well as geomechanical data are available for one well.

3D seismic data acquisition and processing

The acquisition of a 702 mi² (1818 km²) 3D seismic survey spread over Carroll, Tuscarawas, Guernsey, Noble, Belmont, Harrison and Jefferson counties of eastern Ohio (Figure 1), was completed in late 2015. The survey falls in the wet gas and light oil windows of the Utica-Point Pleasant. The acquisition parameters include 220 ft (67.056 m) for source and receiver intervals, 660 ft (201.168 m) for receiver line spacing, 1320 ft (402.336 m) source line spacing, maximum offset as 19,186 ft (5847.89 m), 2 ms sample interval, 5 s record length, which yielded a bin size of 110 ft by 110 ft (33.5 m X 33.5 m). Two vibrator sweeps of 16 s are used as the seismic source. The processing of this large data volume was completed in June 2016, with anisotropic prestack time migration (PSTM) gathers and stacked volume with 5D interpolation made available for reservoir characterization and quantitative interpretation.

Well-log correlation

Correlation of well log information with 3D surface seismic data is a convenient way to extend the measured rock properties at well locations spatially over the 3D volume.

As we started collating well data for our study we realized that the wells that had density curves are located in a cluster to the northern part of the survey, and very few wells had both sonic and density curves. A frequently encountered situation is when not many wells have shear sonic log curves available. It is always desirable to have a uniform location of wells with sonic, density and other curves (GR, porosity, resistivity, etc.) though sparse, as it helps with the generation of a reliable low-frequency impedance model for impedance inversion, as well as for carrying out any neural network analysis for computation of a reservoir property. Besides, any crossplotting carried out on well data located sparsely on a 3D volume, and in localized clusters may not be a true representation of relationships between the crossplotted variables. We therefore selected wells that had an optimum distribution as shown in Figure 2. Some of the wells located at the edge of the 3D survey were projected a little bit inside, as the seismic data close to the edges of the survey are not very trustworthy.

Once the final seismic data are loaded on the workstation, we assessed its quality and frequency content. The data were preconditioned for random noise attenuation by putting it through structure-oriented filtering (Chopra and Marfurt, 2007; Marfurt, 2006).

In Figure 3 we show the correlation of the sonic, density and GR log curves and synthetic seismograms for well W-3 with the seismic data. Five horizons corresponding to Trenton Limestone, Point Pleasant, and Above-Utica in our zone of interest, and Clinton sandstone and Onondaga limestone above it were picked. While the Trenton and Onondaga limestones show good contrast at their levels on the log curves (and thus prominent reflections on seismic), reflections corresponding to Point Pleasant and Clinton sandstone were also pickable. But no individual reflection corresponding to Utica shale could be picked, and so the closest pickable reflection was considered and called 'Above-Utica'. A zero-phase wavelet was extracted from the seismic data using a statistical process (shown on the top) and was used for generating the synthetic seismogram. An overall good correlation is seen between the two.

As shear log curves were available in only three of the eight wells over the 3D survey, that had sonic and density curves, we crossplot the P- and S-impedance for these three wells as shown in Figure 4. The linear relationship seen therein is used to generate the shear curves for five wells that didn't have the shear curves, and then used those seven shear impedance curves (3 measured and 4 predicted using the relationship) for the generation of the low-frequency S-impedance model for inversion. Using the low-frequency model generated with a single well as one of the inputs, and some other seismic data volumes (relative acoustic impedance, instantaneous amplitude, dominant frequency, filtered seismic (10-20-30-40 Hz and 10-20-50-60 Hz), a multiregression approach (Ray and Chopra 2015, 2016) is used, wherein a target log is modeled as a linear combination of several input attributes at each sample point. This approach results in more accurate low-frequency impedance models. Having determined the low-frequency models for both P- and S- impedance, the next step was to carry out preconditioning of the prestack data for enhancing its signal-to-noise ratio. We found that the useable angle range was 34°, and thus the output attributes were P-impedance and S-impedance, but the density attribute could not be determined with simultaneous inversion.

Sweet spot determination

The main goal for shale resource characterization is usually the identification of sweet spots which represent the most favorable drilling targets. Such sweet spots can be picked up as those pockets in the target formation that exhibit *high total organic carbon* (TOC) content, *high porosity*, as well as *high brittleness*. The organic richness in the shale rocks influences properties such as compressional and shear velocities, and density. Therefore, attempts have been made to detect changes in TOC from the surface seismic response using impedance and other attributes such as V_P - V_S ratio, Λ - ρ , μ - ρ etc. (Sharma and Chopra, 2016). In this study we have tried to bring in data from core analysis, as well as geochemical and geomechanical analysis, and integrate that with surface seismic data. The density and TOC measurements made on the core samples in the Point Pleasant interval were crossplotted as shown in Figure 5. A strong linear relationship is seen between them. This suggests that the density attribute would be required if the organic-rich zones in the Point Pleasant interval are to be determined from seismic data.

And as stated above, as the angle range was not favorable for computing density from seismic data through simultaneous inversion, we turned to neural network analysis for its determination. We decided to determine density with probabilistic neural network analysis, employing amongst others some of the attributes determined from simultaneous inversion. Besides the neural network approach followed, the integration of core, geochemical and geomechanical data and seismic data was also carried out. But in Figure 6 we show how the predicted density compares with the measured density at the location of well W-7. The good match between the curves enhanced our confidence in this approach.

Once the density volume was determined from neural network analysis, the linear relationship shown in Figure 5 was used to transform it to a TOC volume. High TOC content was noticed in the northern part of the survey, which is consistent with TOC trend observed in the Utica-Point Pleasant play (Wickstrom, 2013).

Besides the organic richness consideration, it is vital that reservoir zones are sufficiently brittle as fracturing potential of a shale reservoir is a fundamental function of its brittleness. Attempts are usually made to identify the brittle zones with the help of Poisson's ratio and Young's modulus as a rock's ability to fail under stress is represented by the former, while the ability of sustaining fractures is reflected by the latter.

We crossplot Young's modulus and Poisson's ratio for data for wells W-1 and W-7 from the Utica through Point Pleasant to the Trenton interval. We notice a positive correlation between the two parameters and noticed that the Point Pleasant interval exhibits low Young's modulus and Poisson's ratio relative to the Utica interval. As is seen in many other shale formations, brittleness is found to increase as Poisson's ratio decreases and Young's modulus increases (Rickman et al., 2008). Point Pleasant does not seem to follow this behavior, even though the production from the multistage fracking in this interval has been established (Patchen and Carter, 2015). Within the Point Pleasant interval, we see a variation in these two parameters. To study the variation of these parameters within this interval, we restrict the data points coming into the crossplot to just the Point Pleasant interval and see that the cluster of points coming from W-7 (to the south) and the ones coming from W-1 (to the north), Poisson's ratio and Young's modulus both decrease going from north to south.

Grieser and Bray (2007) proposed computing a brittleness average from Young's modulus and Poisson's ratio and demonstrated deciphering brittle and ductile shale pockets within the Barnett shale by considering all values of Poisson's ratio less than 0.25 as threshold and all values of Young's modulus greater than 3.1×10^6 psi.

We follow a similar approach and demonstrate its application to the Utica-Point Pleasant play. Realizing that the Point Pleasant interval has higher calcite content, and therefore its ability to fail under stress and sustain fractures must be high, we picked up the P-impedance and S-impedance derived from simultaneous inversion and density derived from probabilistic neural network analysis to compute Young's modulus and Poisson's ratio attributes. These are then crossplotted just for the Utica to Trenton interval as shown in Figure 7. Notice all points below the value 0.23 for Poisson's ratio (enclosed in red and green polygons) come from the Point Pleasant interval. Thus, we interpret this

interval to be prone to get fractured under stress. The ability of this interval to sustain fractures in a relative sense can be examined based on Young's modulus attribute. It can be seen from Figure 7a that the points enclosed by the green polygon correspond to higher values of Young's modulus, than the points enclosed by the red polygon. When we project these points on the vertical arbitrary line passing through the wells, as exhibited in Figure 7b, we notice that the northern side of this line exhibits higher brittleness than the southern side.

To examine the lateral variation in the Young's modulus we draw a horizon slice from the Young's modulus volume which is shown in Figure 8a. The northern part of the display shows higher values of Young's modulus. Thus, by restricting the values of Poisson's ratio and examining the variation of Young's modulus, we have been able to determine the variation in the brittleness of the Point Pleasant interval. In addition to brittleness, organic richness was also examined through the TOC volume. For doing this we draw an equivalent horizon slice from the TOC volume which is shown in Figure 8b. We notice higher TOC values in the northern part. The areas highlighted in the black polygons are thus the sweet spots that have been determined from the above analysis. This seems accurate enough as confirmed by the available production data overlaid on the TOC display.

So far, the geomechanical properties have been considered for computation of brittleness. However, it is also known that mineralogy plays a vital role in the brittleness of shale formations. Thus, our next step in the workflow was to determine the brittleness of the Point Pleasant formation. The brittleness of a formation is associated with its mineral content (Jarvie et al., 2007). Initially, it was thought that the presence of quartz mineral in a formation makes it more brittle, while more clay makes it ductile. Later, it was observed that the presence of dolomite tends to increase the brittleness of a shale play (Wang and Gale, 2009). Further Jin et al. (2015) note that instead of dolomite, the carbonate contribution (dolomite/calcite) should be considered for computation of brittleness. These authors proposed a brittleness index (*BI*) for identification of brittle zones in a shale play as follows:

$$BI_{mineralogy} = \frac{W_{Quartz} + W_{Calcite} + W_{Dolomite}}{W_{Total}} \quad (1)$$

where *W* corresponds to the weight fraction. Thus, an investigation of different minerals in the zone of interest leads to the identification of favorable drilling zones. Normally, it is an arduous task to compute the individual mineral content of a formation using seismic data, and geoscientists rely on the Young's modulus and Poisson's ratio attributes (Sharma and Chopra, 2015). However, for the present study, the available XRD data suggests that quartz, calcite, and clay are the main minerals present in the Utica play. Additionally, regional petrophysical modeling carried out for the condensate region reveals a strong relationship of clay volume (*V_{clay}*) with the neutron porosity minus density porosity (NMD) data. Furthermore, the quartz group (quartz + feldspar) and the carbonates group (calcite+dolomite) showed a strong relationship with the neutron porosity curve (NPHI). Therefore, the volumes of neutron porosity and density porosity (*DPHI*) should be computed so that the mineralogical content of Utica play can be obtained. For doing so first we crossplot both neutron porosity and density porosity with those attributes from well log data that can be seismically-derived. Thereafter, we select those attributes that show a good correlation, so that the relationship could then be used for transforming the seismically-derived attributes into neutron porosity and density porosity. One such a crossplot between the measured P-impedance and neutron porosity over the Point Pleasant interval is shown in Figure 9. As good correlation is found between P-impedance and NPHI and density and DPHI we use these respective relationships for deriving both NPHI and DPHI volumes from P-impedance and density volumes. A similar analysis is carried out for the Utica interval and we notice a good correlation between DPHI and density, but a better correlation for S-impedance and NPHI. These determined relationships are then used for deriving NPHI and DPHI volumes from inverted P- and S-impedance and density.

Next, the determined relationships discussed above were used to transform the inverted attributes (P-impedance, S-impedance and density) into individual mineral content volume. It was noticed here that more than 40% clay content exists in the Utica interval and it decreases as we go from Utica to Trenton. Quartz group content varies from 20-40% for Utica and Point-Pleasant intervals, being higher in the former than the latter. Additionally, carbonate content decreases as we go from Trenton to Utica interval. Thus, the Point-Pleasant interval contains more carbonate content than the Utica interval and seems to be more brittle. This observation matches well with the available petrographic information for the area of study and lends the confidence in the prediction of different mineral content. With these individual mineral volumes now computed, brittleness index attribute was derived using equation 1. A horizon slice from this mineralogical brittleness index volume over the Point Pleasant interval is shown in Figure 10. Pockets with high values of brittleness are indicated in light blue, dark-blue and magenta colors. The northern part on this display seems to be more brittle, as it exhibits higher values of BI. This observation correlates well with the hydrocarbon production from the Point Pleasant interval, as indicated with the green circles in Figure 8b.

Conclusions

We have characterized the Point Pleasant formation in eastern Ohio using 3D surface and its integration with core, geochemical and geomechanical data. This has been done by deriving rock-physics parameters (Young's modulus and Poisson's ratio) through deterministic simultaneous inversion and neural network analysis. We find that the Point Pleasant formation does not seem to follow the commonly followed variation in terms of low Poisson's ratio and high Young's modulus for brittle pockets. Instead, by restricting the values of Poisson's ratio and examining the variation of Young's modulus, we are able to determine the brittleness behavior within the Point Pleasant interval. Combining the brittleness behavior with the organic richness determined through the TOC content, we are able to pick sweet spots in the Point Pleasant interval which match the production data.

Through this case study, we emphasize the integration of 3D surface seismic data with all other relevant data so as to accurately characterize the Point Pleasant formation.

Acknowledgements

We wish to thank TGS for encouraging this work and also for the permission to present and publish it.



Figure 1: Outline map of Ohio State showing the location of the 3D seismic survey used in the study. The numbers 1 to 7 show the individual counties discussed in the text over which the 3D seismic survey was shot. Overlaid on the outline are the different hydrocarbon phase windows, showing that the survey falls in the wet gas/light oil window. The data for the hydrocarbon phase ribbons was adapted from Mariani (2013).

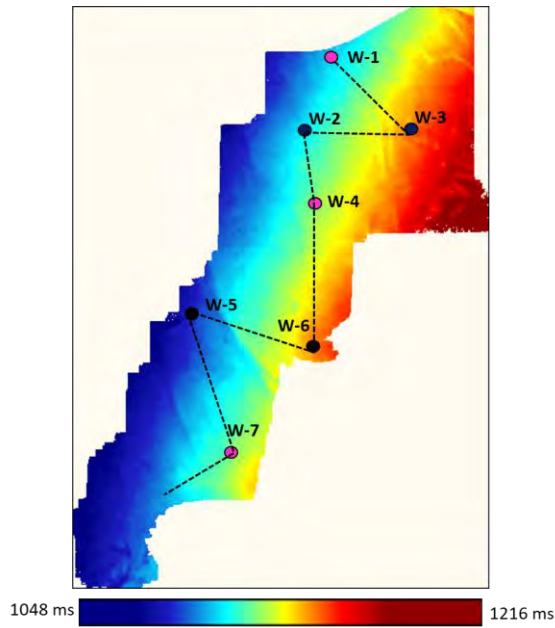


Figure 2: Picked horizon at the Point Pleasant level indicating the dipping reflections from northwest to southeast. The locations of the available wells 1 to 7 are also indicated.

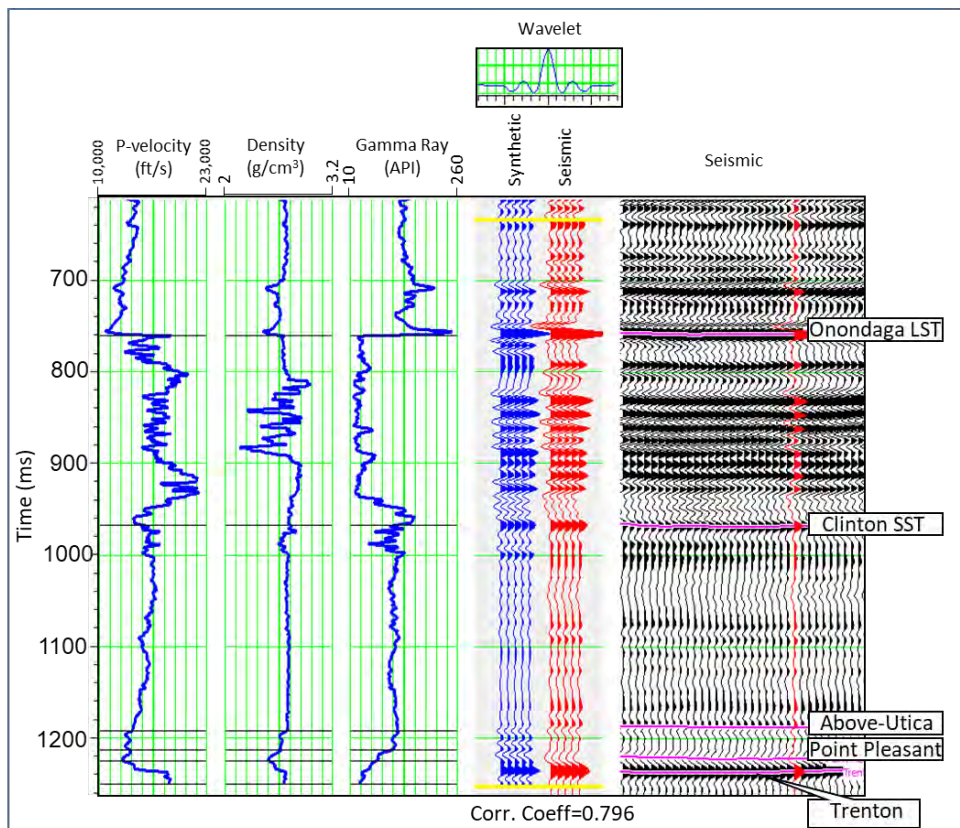


Figure 3: Correlation of well W-3 P-velocity, density and Gamma ray curves with seismic data. Notice the sharp impedance contrast seen at the Onondaga Limestone and Trenton Formation levels giving rise to strong reflections. The horizons corresponding to Onondaga Limestone, 'Clinton' sandstone and Point Pleasant and Trenton levels are pickable and seen clearly on the seismic. (Data courtesy: TGS, Houston)

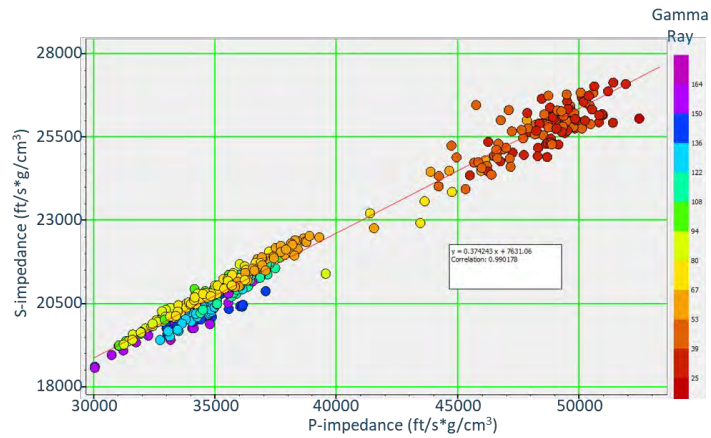


Figure 4: Cross-plot of P-impedance versus S-impedance using well-log data from three wells 1, 4 and 7. A high correlation coefficient is seen for the linear trend observed.

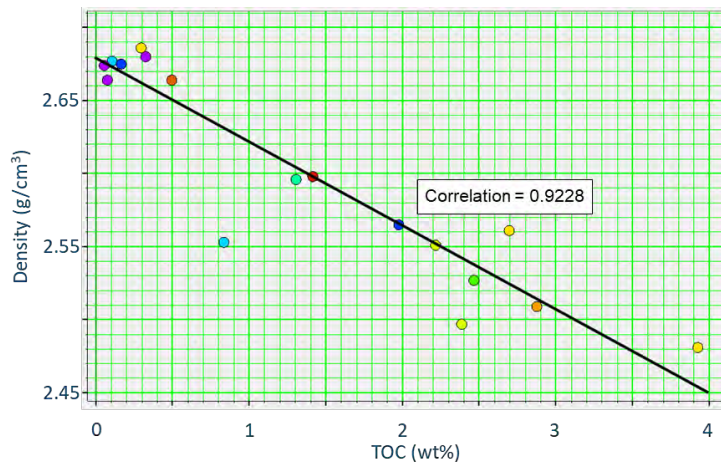


Figure 5: Crossplot of density and weight percent of total organic carbon (TOC) as determined from core data in the Point Pleasant interval. A good linear relationship is seen between the crossplotted variables.

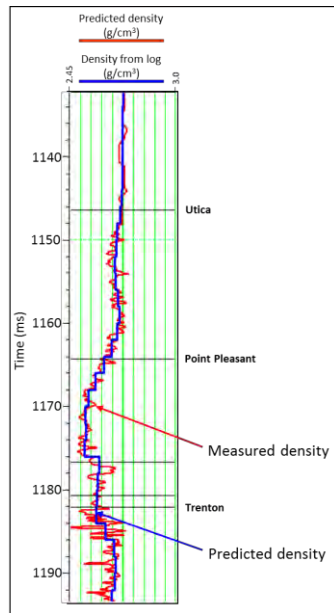


Figure 6: (a) The density trace predicted with neural network application compared with the measured density log curve at the location of well W-7. The two curves overlay well and thus enhance our confidence in neural network density prediction. (b) The derived TOC (wt%) curve shown correlated with the TOC values from the core samples. The good correlation is encouraging.

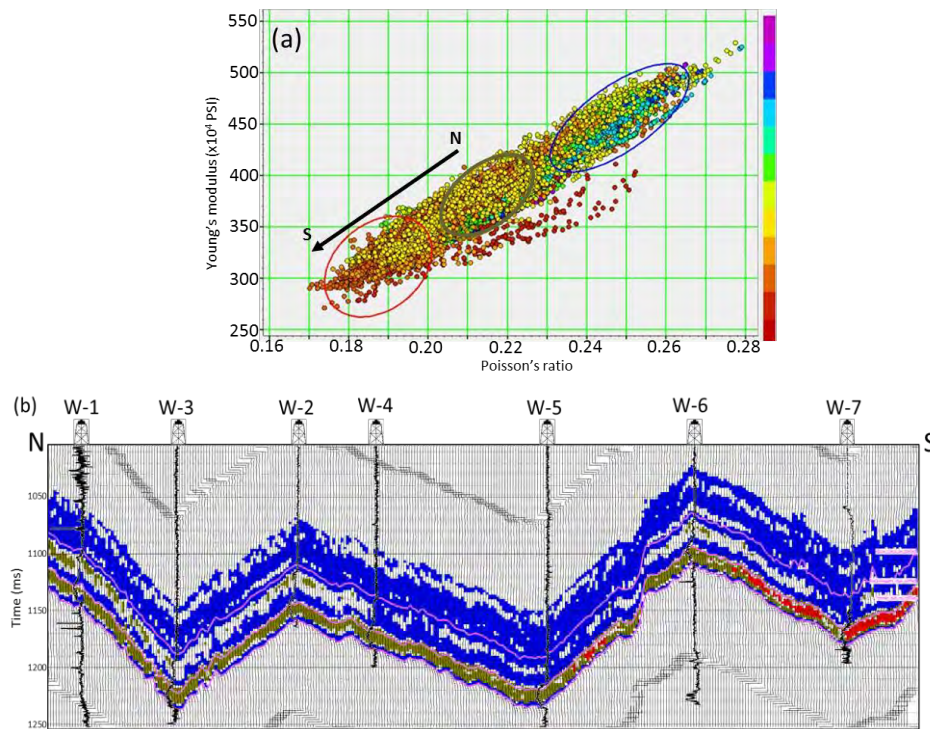


Figure 7: (a) Crossplot between Young's modulus and Poisson's ratio as derived from seismic data for the Utica to Trenton interval. (b) The cluster points in different polygons on the crossplot when projected on the vertical show higher brittleness on the northern side of the survey. (Data courtesy: TGS, Houston)

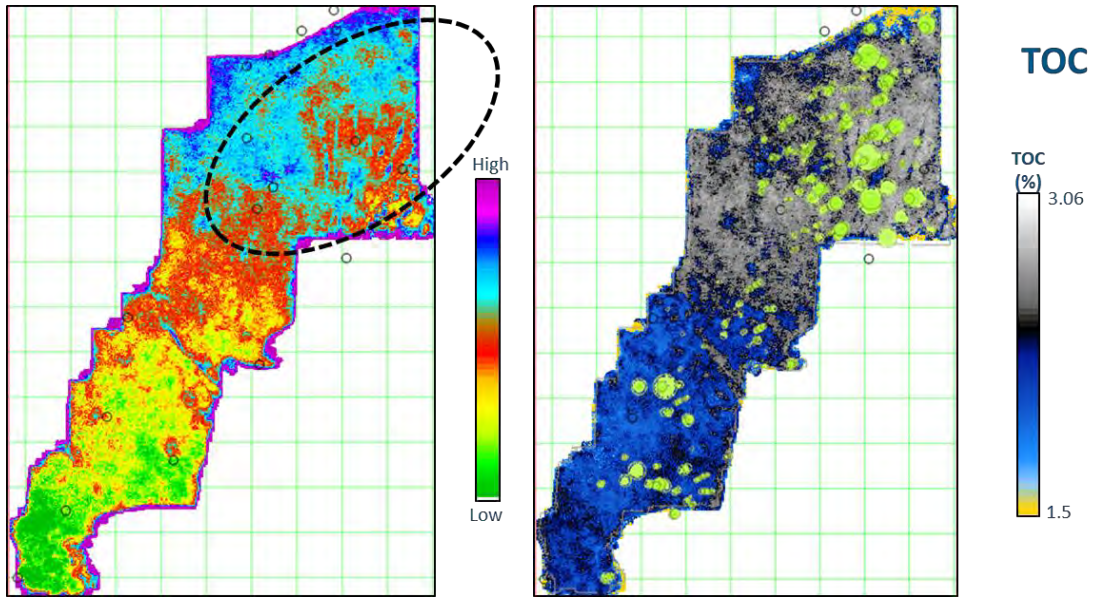


Figure 8: Horizon slices from (a) Young’s modulus, and (b) TOC volumes, both averaged in a 10 ms window in the Point Pleasant interval. The highlighted portions indicate the sweet spots corresponding to high Young’s modulus and high TOC. (Data courtesy: TGS, Houston). Overlaid on the TOC display is the production data. It may be mentioned here that the production data has been obtained from the online open database, and we are not sure about its accuracy. However, the match seems convincing.

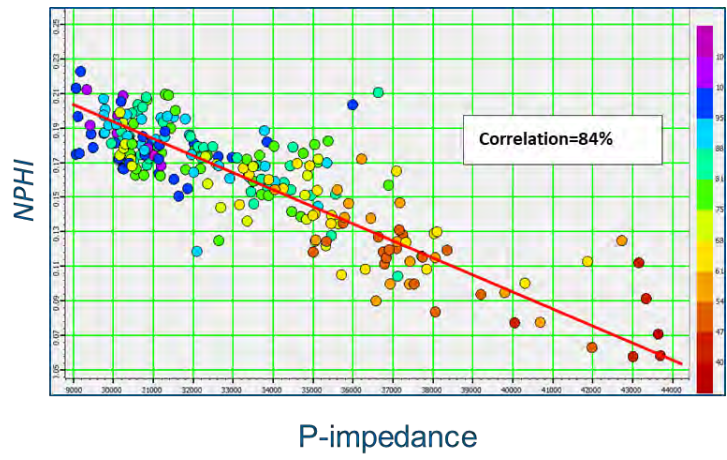


Figure 9: Crossplot of P-impedance versus neutron porosity over the Point Pleasant interval. The good correlation seen suggests that P-impedance can be used to predict neutron porosity. Similarly, the density volume can be used for prediction of density porosity.

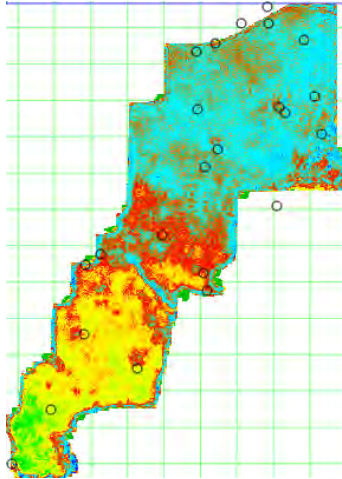


Figure 10: Horizon slice from the mineralogical brittleness index.

References

- Chopra, S., and K. J. Marfurt, 2007, Seismic attributes for prospect identification and reservoir characterization, Geophysical Development Series, SEG.
- Grieser, B., and Bray, J., 2007, Identification of production in unconventional reservoirs: SPE 106623 (SPE Production and Operations. Symposium), Oklahoma City, OK, March 31-April 3, 2007.
- Cocklin, J., 2015: Shale Daily, published on July 14., 2015, available at (<http://www.naturalgasintel.com/articles/102982-wvu-study-finds-bounty-of-utica-shale-natgas-waiting-for-production>) and accessed on February 18, 2017.
- Jarvie, D.M., R.J. Hill, T.E. Ruble and R.M. Pollastro, 2007, Unconventional shale-gas systems: the Mississippian barnett shale of north-central Texas as one model for thermogenic shale-gas assessment: AAPG Bulletin. 91 (4) 475-499.
- Jin, X., S.N. Shah and J.C. Roegiers, 2015, An Integrated Petrophysics and Geomechanics Approach for Fracability Evaluation in Shale Reservoirs: June SPE Journal, 518-526.
- Kirschbaum, M.A., C. J. Schenk, T. A. Cook, R. T. Ryder, R. R. Charpentier, T. R. Klett, S. B. Gaswirth, M. E. Tennyson, and K. J. Whidden, 2012, Assessment of undiscovered oil and gas resources of the Ordovician Utica Shale of the Appalachian Basin Province, 2012: U.S. Geological Survey Fact Sheet 2012–3116, 6.
- Marfurt, K. J., 2006: Robust estimates of reflector dip and azimuth: Geophysics, **71**, P29-P40.
- Patchen, D.G. and K. M. Carter, eds., 2015, A geologic play book for Utica Shale Appalachian basin exploration, Final report of the Utica Shale Appalachian basin exploration consortium, 187 available at: <http://www.wvgs.wvnet.edu/utica> and accessed on 18th February, 2017.
- Ray, A. K. and S. Chopra, 2015, More robust methods of low-frequency model building for seismic impedance inversion, 85th Annual International Meeting, SEG, Expanded Abstracts, 3398-3402.
- Ray, A. K. and S. Chopra, 2016, Building more robust low-frequency models for seismic impedance inversion: First Break, **34**, 29-34.
- Rickman, R., M. J. Mullen, J. E. Petre, W. V. Grieser, and D. Kundert, 2008, A Practical Use of Shale Petrophysics for Stimulation Design Optimization: All Shale Plays Are Not Clones of the Barnett Shale. SPE 115258, Society of Petroleum Engineers.

Sharma, R. K. and S. Chopra, 2016, Identification of sweet spots in shale reservoir formations: First Break, **34**, 39-47.

Wang, F.P and J.F. Gale, 2009, Screening criteria for shale-gas system: Gulf Coast Asso. Geol. Soc. Trans. 59 779-793.

Wickstrom, L., 2013, Geology and activity of the Utica-Point Pleasant of Ohio, http://www.searchanddiscovery.com/documents/2013/10490wickstrom/ndx_wickstrom.pdf and accessed on 18th February, 2017.